Algorithms & Hardware Inc.

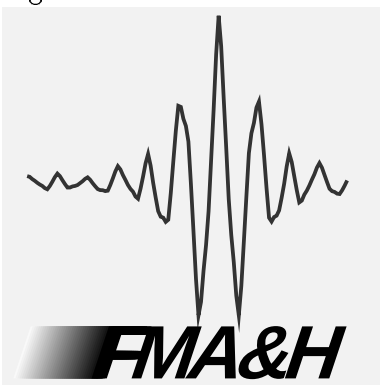


Mathematics Department


# The Xwpl system Reference Manual

for version 1.3 of Xwpl

Fazal Majid **(majid@math.yale.edu)**,
Ronald R. Coifman, M. Victor Wickerhauser

December 10, 1993

# Contents

# List of Figures

# Chapter 1

# Introduction

## 1.1 What is Xwpl

Xwpl is a graphical tool to analyse one-dimensional signals using adapted waveform analysis, under the X Window System.

Wavelets, wavelet packets and local trigonometric waveforms are collections of short oscillatory waveforms each of which can be viewed as a "musical note" having a time duration, a pitch and an amplitude (level of loudness). The waveforms used here are synthesized mathematical notes, as synthesized by different mathematical instruments (corresponding to different processes used to generate the notes).

To pursue the musical analogy further, Xwpl displays the "musical score" for a signal using the *Phase Cell representation*, in which a "note" (a function in the wavelet or wavelet-packet basis) is represented by a box in the time-frequency space (time is horizontal, frequency is vertical). The boxes all have the same area as a result of Heisenberg's inequality on fourier transforms. See A.3.1 for more details on how this representation should be interpreted.

For instance, the signal in figure 1.1 is a chirp of the form $y = sin(at^2)$, which is difficult to analyse using classical fourier theory, as it's instantaneous frquency varies with time (as a matter of fact, even the graphical representation is deceived into showing a signal with a varying envelope).

Figure 1.2 shows a "musical transcription" of the same chirp using a "C 12" *Quadrature Mirror Filter* or QMF. This representation shows clearly that the local frequency of the signal increases linearly with time. The dark-

Figure 1.1: A chirp

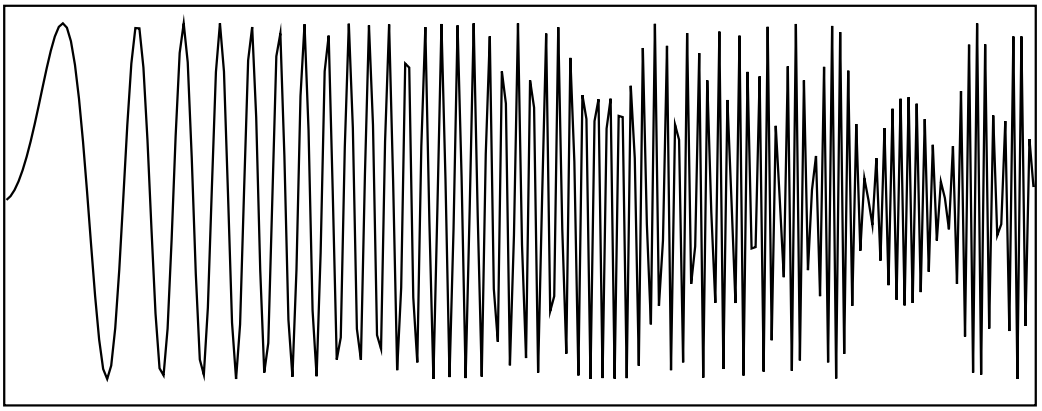

ness of each box is proportional to the intensity of the corresponding wavelet-packet coefficient. Actually, the whole square is filled with boxes, but most of the coefficients are so small or even zero that thay do not appear on the graph.

There are three type of bases when using wavelet packets: best-basis, best-level and wavelet basis. They are described in more detail later, but suffice to to say that they differ in the constraints that are placed on the shape of the boxes. In this case, the best-level basis is the same as the best-basis, but this is not necessarily the case.

Figure 1.2: Best-basis representation of the chirp

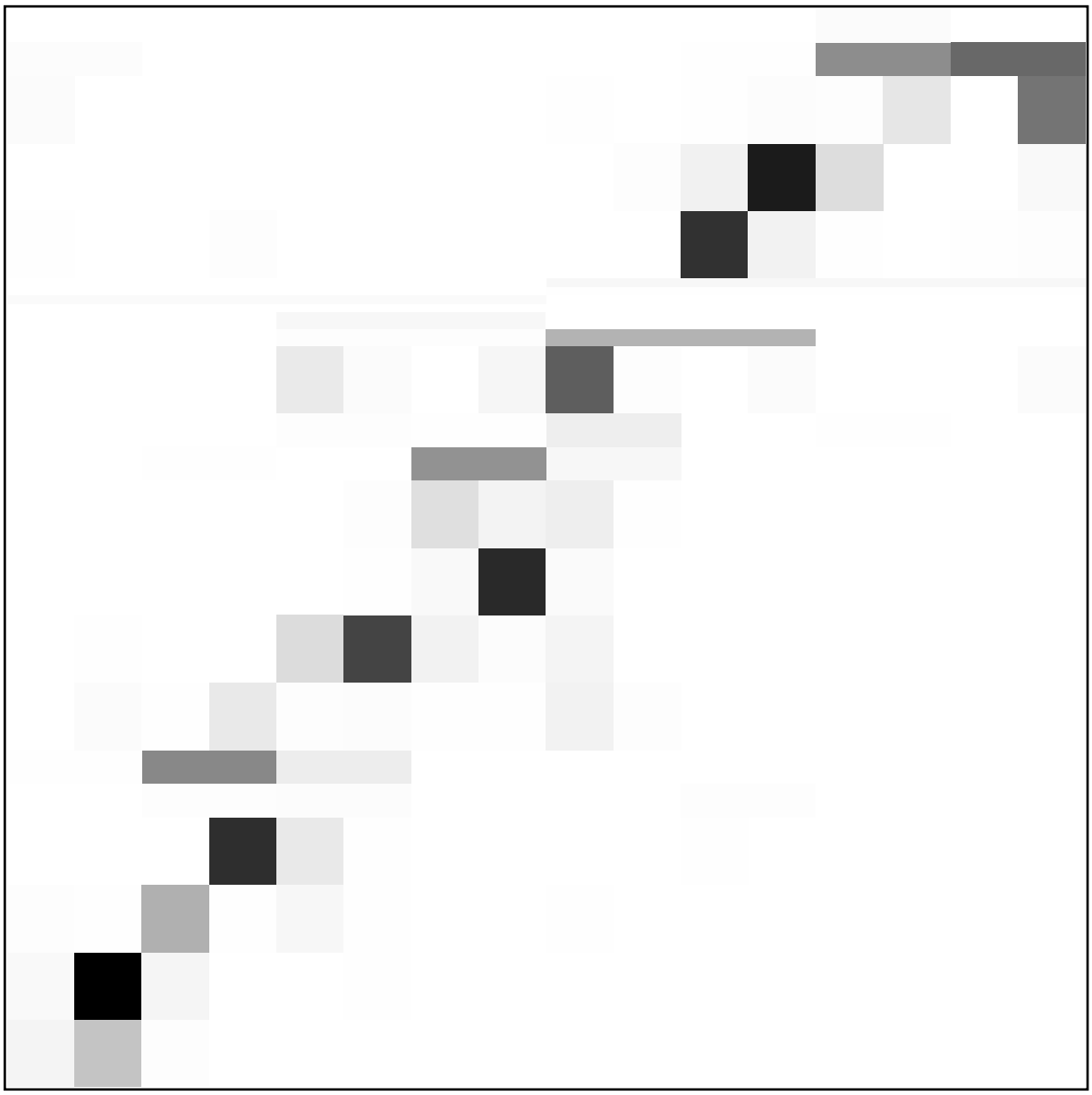

Figure 1.3: Wavelet basis representation

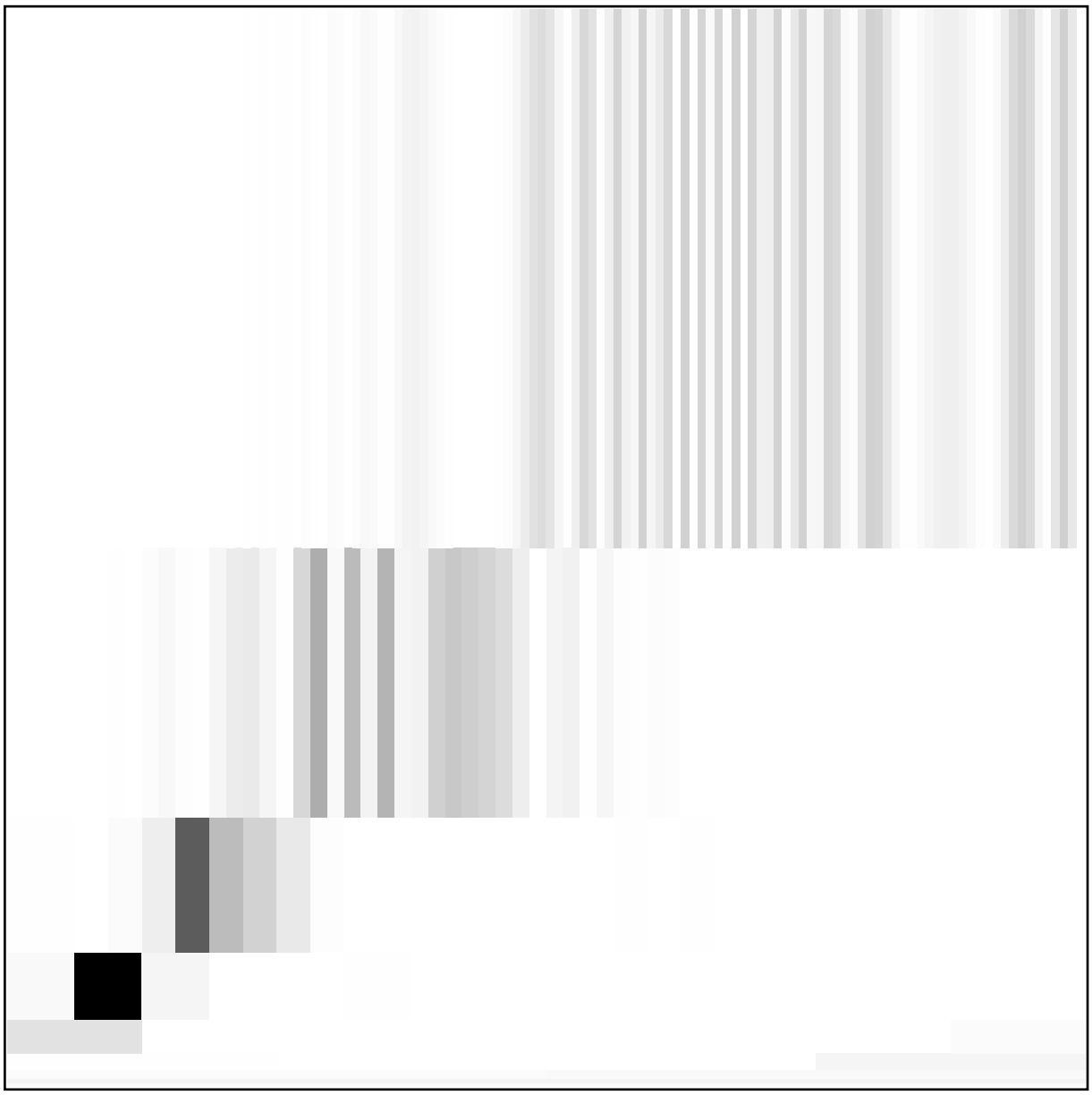

# Chapter 2

# Quick Start

## 2.1 Getting started with Xwpl

### 2.1.1 Invoking Xwpl

Xwpl is invoked by simply typing the command "Xwpl" in a shell. If the program is not found, verify that it is in your `PATH` environment variable. If you get a message of the form: "`Error: Can't open display: foo:0.0`", check to see if your `DISPLAY` environment variable is correctly set. In most cases, a value of "`:0.0`" should be sufficient.

### 2.1.2 The Xwpl main window

The window in figure 2.1 should appear in your display (with variations according to your local application defaults and X resources, if any).

The windows and controls are, going downwards and from left to right:

- `Open` button
- `Save` button
- `Quit` button
- `Info` button
- QMF list

Figure 2.1: Xwpl main window

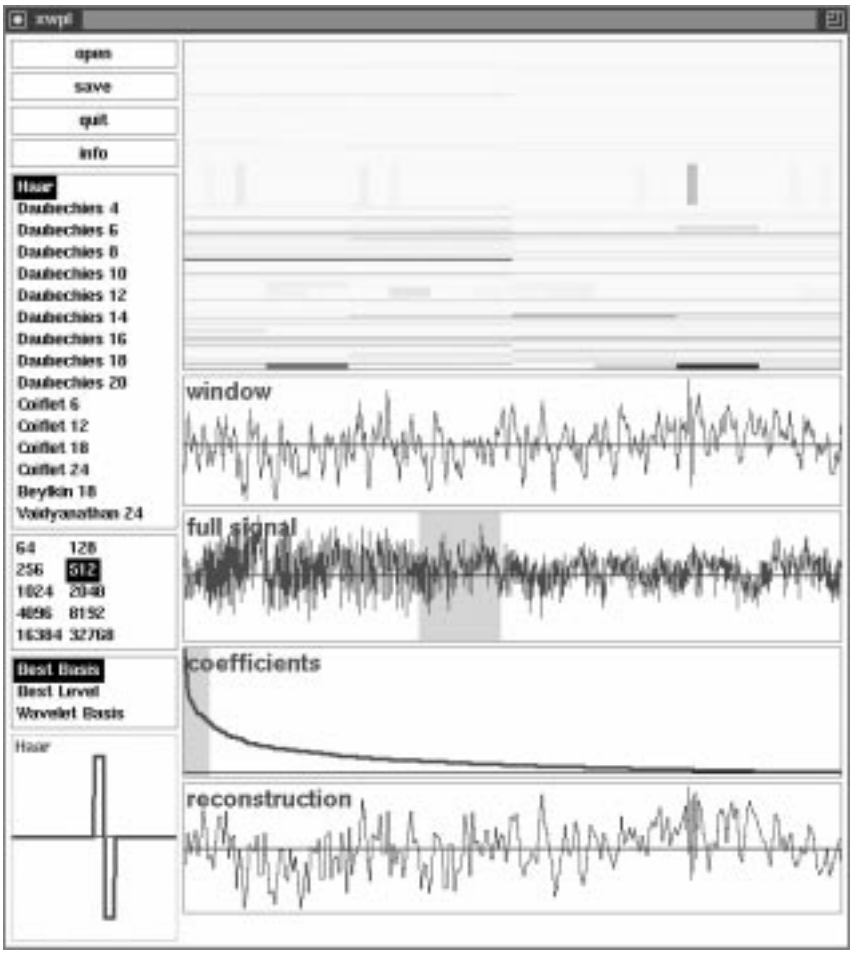

- signal window width list
- bases list
- QMF box
- `Play` button (shown only on machines where sound is supported)
- phase representation box
- signal window plot
- full signal plot
- coefficients plot
- reconstructed signal plot

### 2.1.3 Opening a data file

To open a data file, click on the `Open` button. The dialog box of figure 2.2 will appear. The data file must be an ASCII text file containing floating-point numbers in decimal or scientific notation, separated by newlines or some other whitespace. This representation is inefficient, but highly portable, and lends itself well to treatment by standard Unix utilities such as `awk(3)`.

The file selection dialog is designed to mimic the Macintosh™ browser.

## 2.2 Changing the transformation settings

By default, the QMF used for transformations is the Haar (or D2) filter. The filters can be changed using the QMF list (on the left of the program window). The mother wavelet corresponding to the selected filter is displayed in the QMF box.

The three different types of bases can be changed with the bases list (also on the left-hand side of the Xwpl window).

Figure 2.2: File Browser

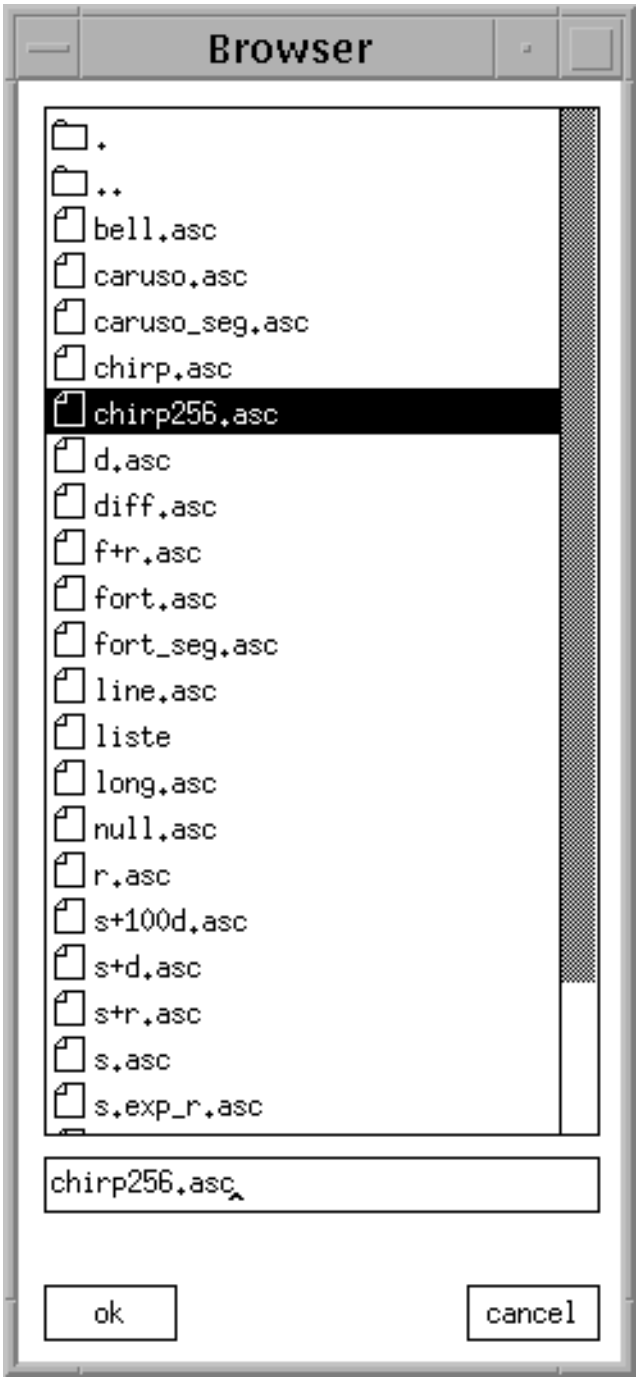

## 2.3 Zooming control

There are three different ways of zooming into a portion of the signal. These are:

- Selecting a portion of the full signal plot. This will cause the signal window to zoom into the desired portion of the signal (to the nearest power of 2).
- Selecting a portion of the windowed signal plot, which has the same effect as the previous method
- Selecting a width from the widths list. This selects a window of the desired width, approximatively centered at the same point as the previous selection (unless that would cause the window to overstep the original signal, in which case it is translated to fit)

To zoom out, simply select a larger window in the full signal plot.

As you zoom, the widths list is updated to reflect the current window width.

## 2.4 Denoising control

To denoise a signal, one keeps a portion of the signal's coefficients in the selected basis, and reconstructs from these coefficients. Xwpl has an algorithm to predict where to make this cut. This is displayed graphically in the coefficient plot (showing the sorted amplitudes of the coefficients). By selecting another portion of the coefficients, the user can do a different kind of denoising.

The reconstructed signal can be saved into a file by clicking on the `Save` button. Only the current reconstructed window is saved.

## 2.5 Program Information

Clicking on the Info button displays information on the program. Click on it again to make it disappear. Some of the information displayed is:

- the program version and build date
- the program copyright information.

# Chapter 3

# Troubleshooting

**Problem 1** *I am running Solaris (SunOS 5.x), and the Sun4 version of XWPL doesn't work.*

Solaris and SunOS 4.1.x are not compatible. I'll put out a Solaris version when I see a usable version of Solaris.

**Problem 2** *On my NeXT computer, XWPL aborts after a message "*`Error: Can't open display:`*".*

XWPL is an X Window System application, not a NeXTstep one. You need a NeXT X server to run it. Due to poor NeXTstep 3.1 Posix conformance, the NeXT port is on hold indefinitely. Otherwise, you could use the WPLab program, which is NeXTstep-based. It is available from wuarchive.wustl.edu in the directory /doc/techreports/wustl.edu/math/software.

**Problem 3** *The colors in the phase box are a day-glo nightmare.*

XWPL tries to be a "good citizen" by not agressively grabbing colors from the colormap. If you have a colormap hog running (graphics display or fancy background screens, for instance), they will interfere with it. Quit your color-intensive applications and/or restart your X server.

**Problem 4** *On my Silicon Graphics workstation, the phase diagram is wishy-washy or even invisible, and the colors are hard to see.*

This problem is due to the special graphics hardware and colormap situation on 24-bit SGI workstations. You must use the **`palette`**, **`showmap`**, **`interp`** commands to adjust your colormap.

**Problem 5** *I have added a file to the directory from which XWPL is reading, but it doesn't appear.*

The XWPL file browser does not poll to see if the contents of the directory have been updated. To do so, simply double-click on the  directory to re-read the current directory.

**Problem 6** *XWPL crashes with a BadAlloc error.*

You have run out of memory...

# Chapter 4

# Installing Xwpl

## 4.1 Requirements

Xwpl works on a workstation using the UNIX operating system (or any system conforming to the IEEE Posix P1003.1 standard) and using the X Window System as a windowing environment. Building it requires an ANSI C compiler and the widely available MIT Athena widget set library (or a compatible library such as Xaw3D).

The use of Xwpl requires a run-time license for the AWA library of M.V. Wickerhauser (also available from FMA&H Inc.). Building Xwpl requires the `libawa.a` library. Xwpl has been built on X11R4 and X11R5 systems.

Xwpl has been built and tested on the following platforms:

Figure 4.1: List of tested systems

| Machine | Operating System | Compiler | X Libraries |
|---|---|---|---|
| Sun SparcStation 2 | SunOS 4.1.1 | gcc 2.4.5 | X11R4 and Xaw |
| i486 PC | Linux 0.99pl10 | gcc 2.3.3, libc 4.3.3 | X11R5 (Xfree86 1.2) and Xaw3D |
| SGI Iris 4D/GT | Irix 4.0.1 | SGI C | X11R4 and Xaw |
| DEC 3000/300 AXP | DEC OSF/1 1.3a | DEC C (c89) or DEC C++ (cxx) | Xdec (R5) and Xaw |
| HP PA-RISC | HP-UX 9.0 | HP c89 | X11R5 and Xaw |

# Appendix A

# Mathematical background

## A.1 Waveform Libraries

We start by recalling the concept of a "Library of orthonormal bases". For the sake of exposition we restrict our attention to two classes of numerically useful waveforms, introduced recently (cf. [5][7]).

### A.1.1 Local trigonometric bases

We start with trigonometric waveform libraries. These are localized sine transforms (LST) associated to covering by intervals of $\mathbb{R}$ (more generally, of a manifold).

We consider a cover $\mathbb{R} = \bigcup_{-\infty}^{+\infty} I_i$, with $I_i = [\alpha_i, \alpha_{i+1})$ and $\alpha_i < \alpha_{i+1}$, write $\ell_i = \alpha_{i+1} - \alpha_i = |I_i|$ and let $p_i(x)$ be a window function supported in $[\alpha_i - \ell_{i-1}/2, \alpha_{i+1} + \ell_{i+1}/2]$ such that

$$\sum_{-\infty}^{\infty} p_i^2(x) = 1$$

and

$$p_i^2(x) = 1 - p_i^2(2\alpha_{i+1} - x) \quad \text{for x near} \quad \alpha_{i+1}$$

then the functions

$$S_{i,k}(x) = \frac{2}{\sqrt{2\ell_i}} p_i(x) \sin\left[(2k+1)\frac{\pi}{2\ell_i}(x - \alpha_i)\right]$$

form an orthonormal basis of $L^2(\mathbb{R})$ subordinate to the partition $p_i$. The collection of such bases forms a library of orthonormal bases (cf. [7]).

It is easy to check that if $H_{I_i}$ denotes the space of functions spanned by $S_{i,k},\ k = 0, 1, 2, ...$ then $H_{I_i} + H_{I_{i+1}}$ is spanned by the functions

$$P(x)\frac{1}{\sqrt{2(\ell_i + \ell_{i+1})}} \sin\left[(2k+1)\frac{\pi}{2(\ell_i + \ell_{i+1})}(x - \alpha_i)\right]$$

where

$$P^2 = p_i^2(x) + p_{i+1}^2(x)$$

is a "window" function covering the interval $I_i \cup I_{i+1}$.

### A.1.2 Wavelets and Wavelet Packets

We consider the frequency line $\mathbb{R}$ split as $\mathbb{R} = \mathbb{R}^+ \cup \mathbb{R}^-$, with $\mathbb{R}^+ = (0, \infty)$ and $\mathbb{R}^- = (-\infty, 0)$. On $L^2(0, \infty)$ we introduce a window function $p(\xi)$ such that $\sum_{k=-\infty}^{\infty} p^2(2^{-k}\xi) = 1$ and $p(\xi)$ is supported in $(3/4, 3)$. We can clearly view $p(2^{-k}\xi)$ as a window function over the interval $(2^k, 2^{k+1})$ and observe that

$$s_{k,j} = \sin\left[\left(j + \frac{1}{2}\right)\pi\left(\frac{\xi - 2^k}{2^k}\right)\right] p(2^{-k}\xi)$$

form an orthonormal basis of $L^2(\mathbb{R}^+)$. Similarly

$$c_{k,j} = \cos\left[\left(j + \frac{1}{2}\right)\pi\left(\frac{\xi - 2^k}{2^k}\right)\right] p(2^{-k}\xi)$$

gives another basis, whose elements are not orthogonal to those of the first one. If we define $S_{k,j}$ as an odd extension to $\mathbb{R}$ of $s_{k,j}$ and $C_{k,j}$ as an even extension we find $s_{k,j} \perp C_{k',j'}$ permitting us to write $C_{k,j} \pm iS_{k,j} = e^{\pm ij\pi\xi/2^k}\hat{\psi}(\xi/2^j)$ where $\hat{\psi}(\xi) = e^{i\pi/2\xi}p(\xi)$ is the Fourier transform of the wavelet $\Psi$ (cf. [4]).

Thus, wavelet analysis corresponds to windowing frequency space in "octave" windows $(2^k, 2^{k+1})$.

A natural extension is provided by allowing all dyadic windows in frequency space and adapted window choice. This sort of analysis is equivalent to wavelet packet analysis.

Figure A.1: LCT

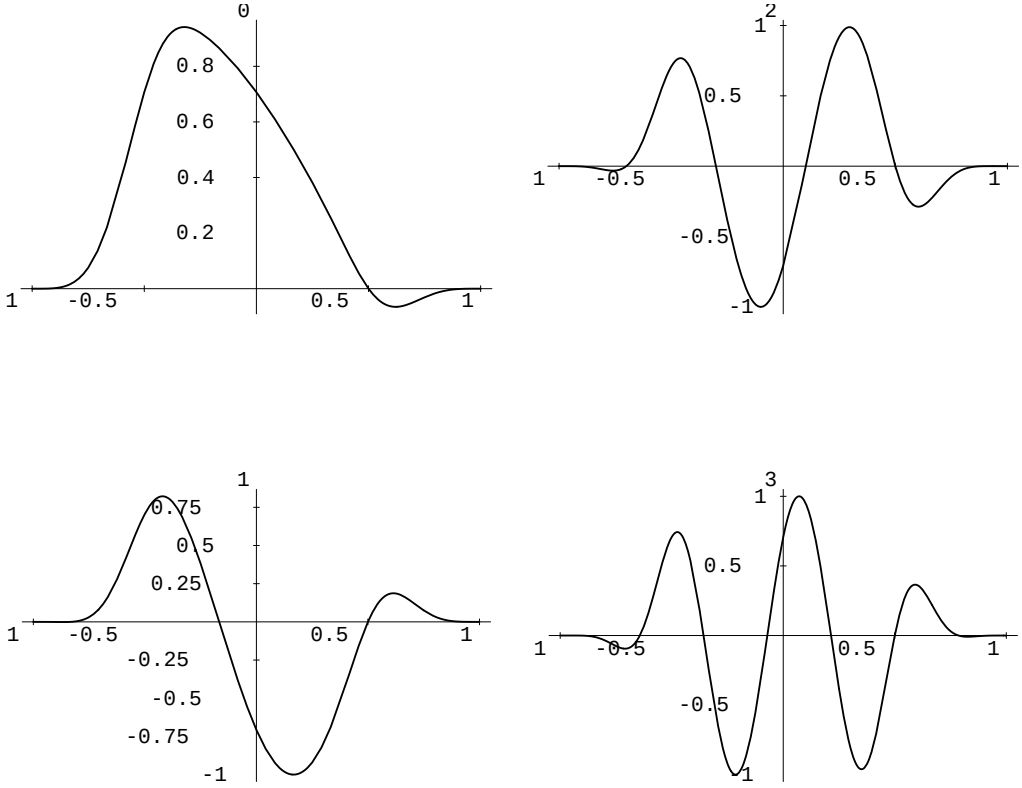

The actual fast wavelet packet analysis algorithms (wavelets being a special cases) permit us to perform an adapted Fourier windowing directly in time domain by successive filtering of a function into different regions in frequency. The dual version of the window selection provides an adapted subband coding algorithm.

The wavelet packet library is constructed by iterating the wavelet algorithm. This library contains the wavelet basis, Walsh functions, and smooth versions of Walsh functions called wavelet packets (cf. [5])

These waveforms are mutually orthogonal. Moreover, each of them is orthogonal to all of its integer translates and dyadic rescaled versions. The full collection of these wavelet packets (including translates and rescaled versions) provides us with a library of "templates" or "notes" which are matched "efficiently" to signals for analysis and synthesis (cf. [2]), Wavelet packet expansions correspond algorithmically to subband coding schemes and are numerically as fast as the FFT.

## A.2 Entropy considerations

We will now measure the distance or good fit between a basis and a function in terms of the Shannon entropy of the expansion.

Let $H$ be a Hilbert space.

Let $v \in H$, $\|v\| = 1$ and let $H = \oplus \sum H_i$ be an orthogonal decomposition of $H$. We define

$$\varepsilon^2(v, \{H_i\}) = -\sum \|v_i\|^2 \ln \|v_i\|^2$$

the entropy of $v$ relative to the decomposition $\{H_i\}$ of $H$, as a measure of the distance between $v$ and the orthogonal decomposition.

$\varepsilon^2$ is characterized by the Shannon equation, which is a version of Pythagoras' theorem. Let

$$H = (\sum H_i) \oplus (\sum H_j) = H_+ \oplus H_-$$

i.e. $H_i$ and $H_j$ give orthogonal decompositions $H_+ = \sum H_i$, $H_- = \sum H_j$.

Then

$$\begin{aligned} \varepsilon^2(v, \{H_i, H_j\}) = \quad & - \frac{\|v_+\|^2}{\|v\|^2} \ln \left( \frac{\|v_+\|^2}{\|v\|^2} \right) - \frac{\|v_-\|^2}{\|v\|^2} \ln \left( \frac{\|v_-\|^2}{\|v\|^2} \right) \\ & + \|v_+\|^2 \varepsilon^2 \left( \frac{v_+}{\|v_+\|}, \{H^i\} \right) + \|v_-\|^2 \varepsilon^2 \left( \frac{v_-}{\|v_-\|}, \{H_j\} \right) \end{aligned}$$

Figure A.2: Wavelet-packets

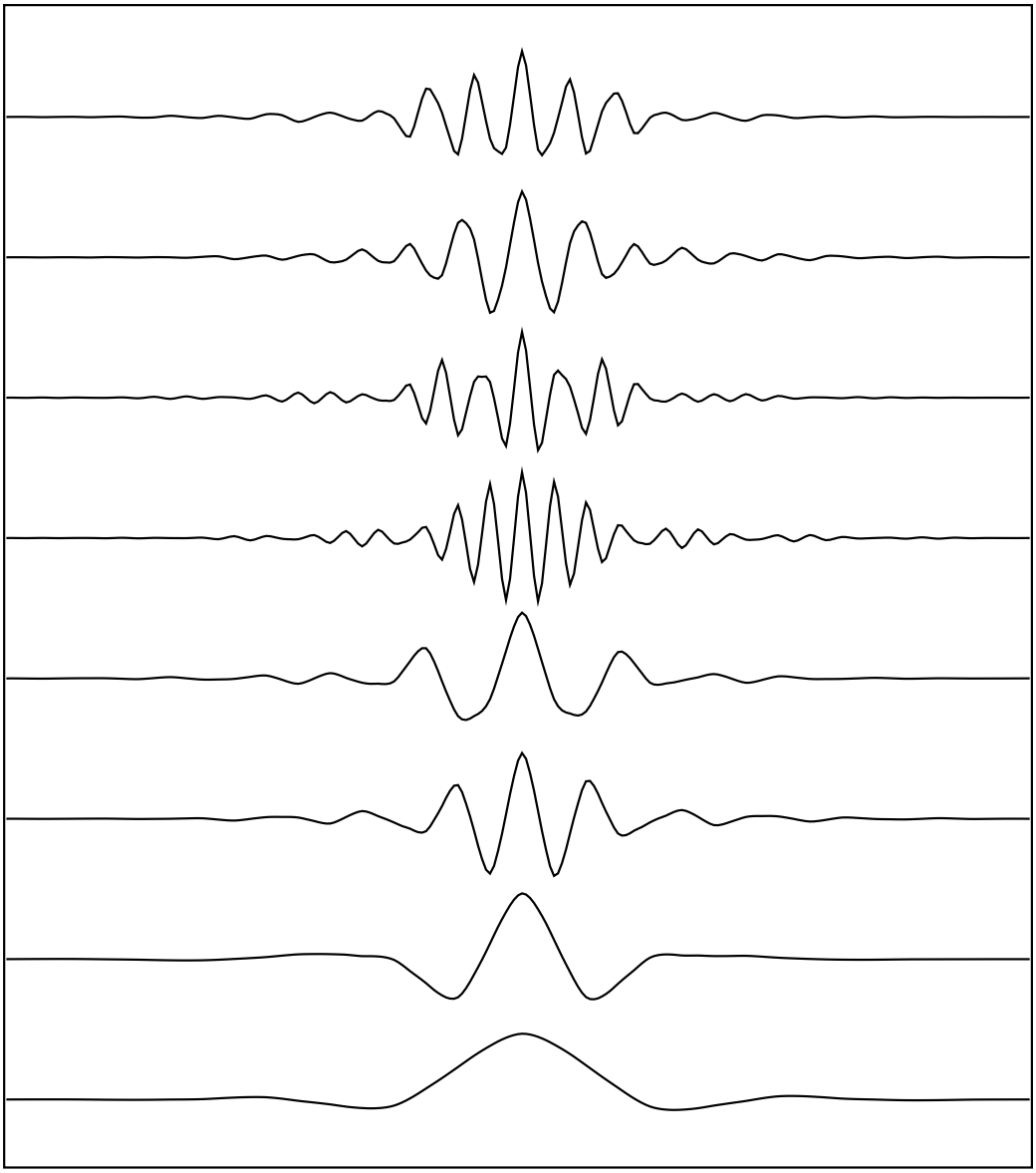

Figure A.3: Tree search In the LST library

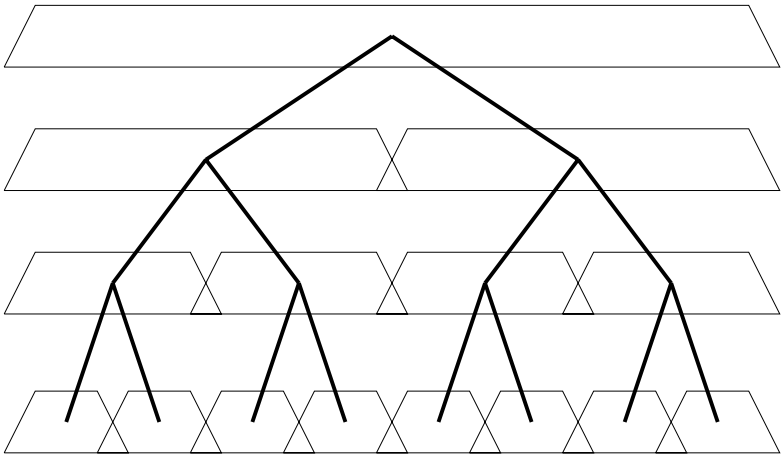

b(x) sin[(k+1/2)(x-a)/L]

a - endpoint ,
L -length

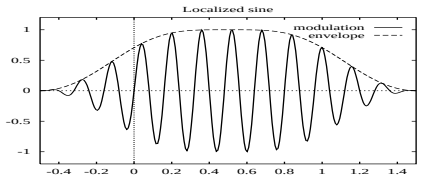


This is Shannon's equation for entropy (if we interpret as in quantum mechanics $\|P_{H_+} v\|^2$ as the "probability" of $v$ to be in the subspace $H_+$).

This equation enables us to search for a smallest entropy expansion of a signal.

For example in the LST Library case, we compare the entropy of the expansion in two adjacent windows to the entropy of the expansion on their union and pick the least expensive, continuing the comparison with the selection made for the next pair, etc. (cf. figure A.3).

## A.3 Time-Frequency Analysis

### A.3.1 The phase cell representation

To each wavelet packet or local trigonometric function we can associate a time $t$ and a frequency $f$. These will be uncertain by amounts $\Delta t$ and $\Delta f$, respectively. The result may be interpreted as a rectangular patch of dimensions $\Delta t$ by $\Delta f$, located around $(t, f)$. We shall call the patch a *phase cell*, or Heisenberg box, in honor of the uncertainty principle, which limits how small the area of the patch may be. The cells may be colored in proportion to the amplitude of the corresponding wavelet packet component.

An orthonormal basis corresponds to a disjoint cover of the phase plane by phase cells (Heisenberg boxes). Certain bases have characterizations in terms of the shapes of the boxes present in the cover. For example, the standard basis consists of the cover by the tallest, thinnest patches allowed by the sampling interval. The Fourier transform may be regarded as the transpose of the standard basis, in the sense that the cells are transposed by interchanging time and frequency (cf. figure A.5). The standard basis has optimal time localization and no frequency localization, while the Fourier basis has optimal frequency localization, but no time localization.

Windowed Fourier or cosine transforms with a fixed window size correspond to covers with congruent cells whose width $\Delta t$ is the window width. The ratio of frequency uncertainty to time uncertainty is the aspect ratio of the cells.

The wavelet basis is an octave-band decomposition of the phase plane, as in figure A.7.

The best-basis of wavelet packets fits a cover to the signal so as to minimize the amount of dark phase cell boxes. The compressibility of a sampled signal is easily seen to be the ratio of the total area of the phase plane ($N \times N$ for a signal sampled at $N$ points) divided by the total area of the dark cells (each of area $N$). This method allows rectangles of all aspect ratios. The best-level or adapted subband basis fits a cover of equal aspect ratio rectangles to the signal, so as to minimize the amount of dark. We may automatically analyze signals by expanding them in the best basis, then drawing the corresponding phase plane representation. As is clear, the negligible components will not be drawn, as it is not relevant which particular basis is chosen for a subspace containing negligible energy.

Figure A.4: Cells in the Phase Plane.

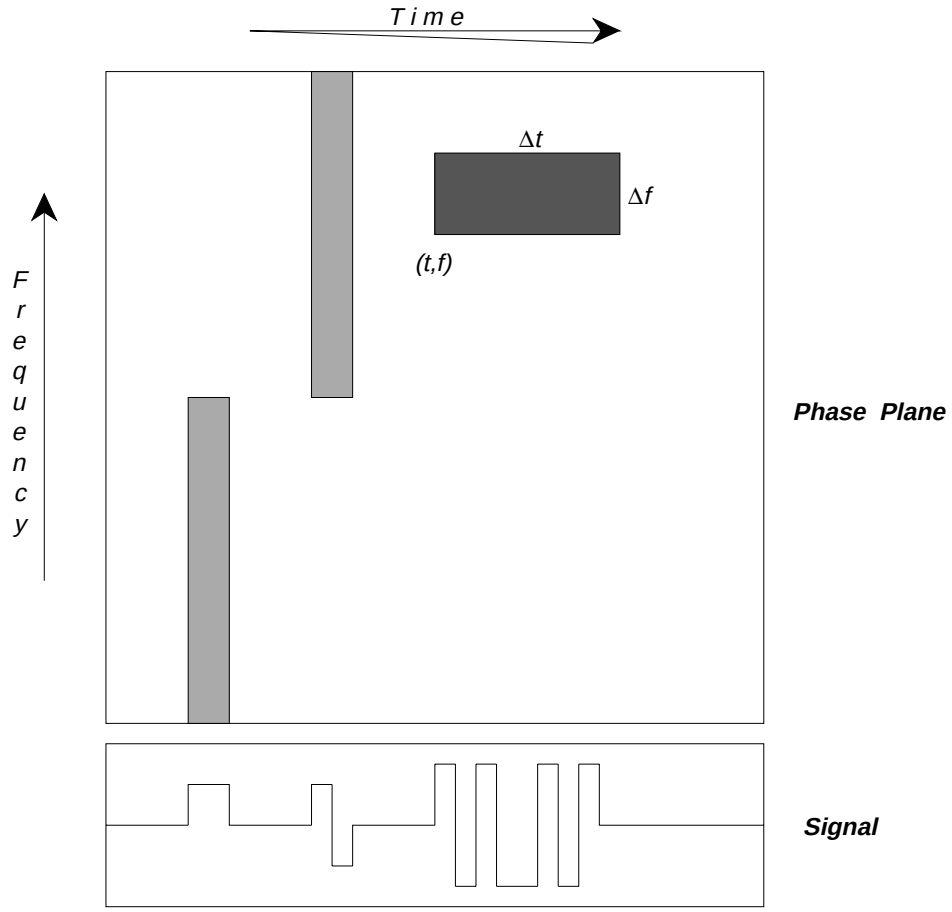

Figure A.5: Phase Plane Decomposition by the Standard and Fourier Bases.

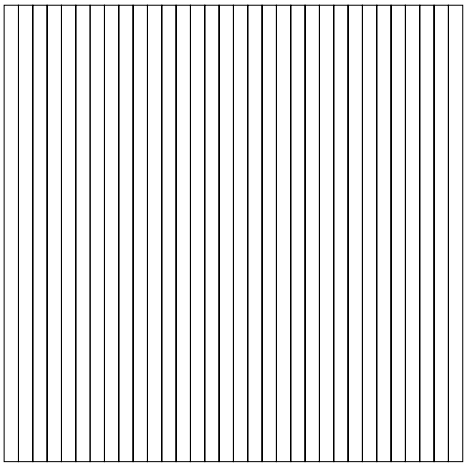

Standard Basis

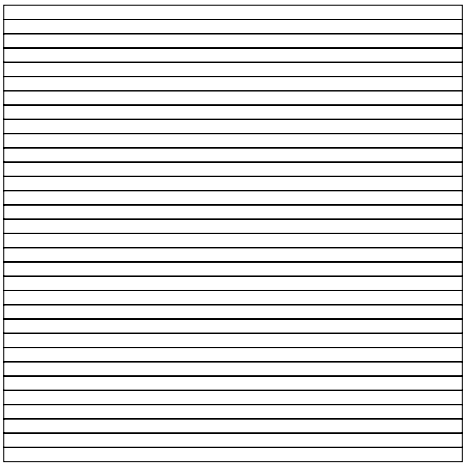

Fourier Basis

Figure A.6: Phase Plane Decomposition by Windowed Cosine Transforms.

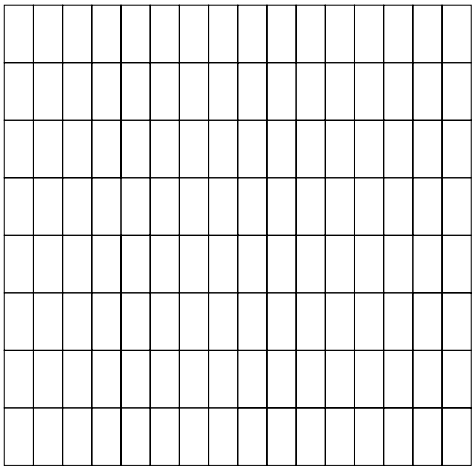

Narrow windows

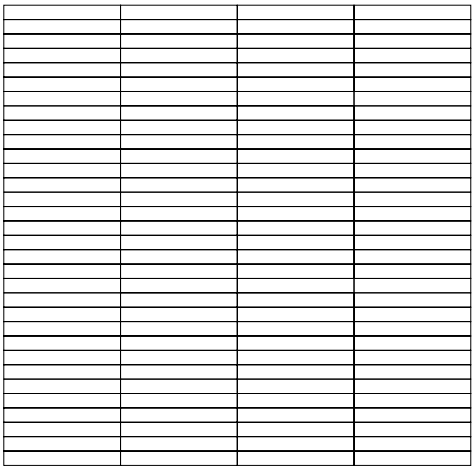

Wide windows

Figure A.7: Phase Plane Decomposition by Wavelet Transform.

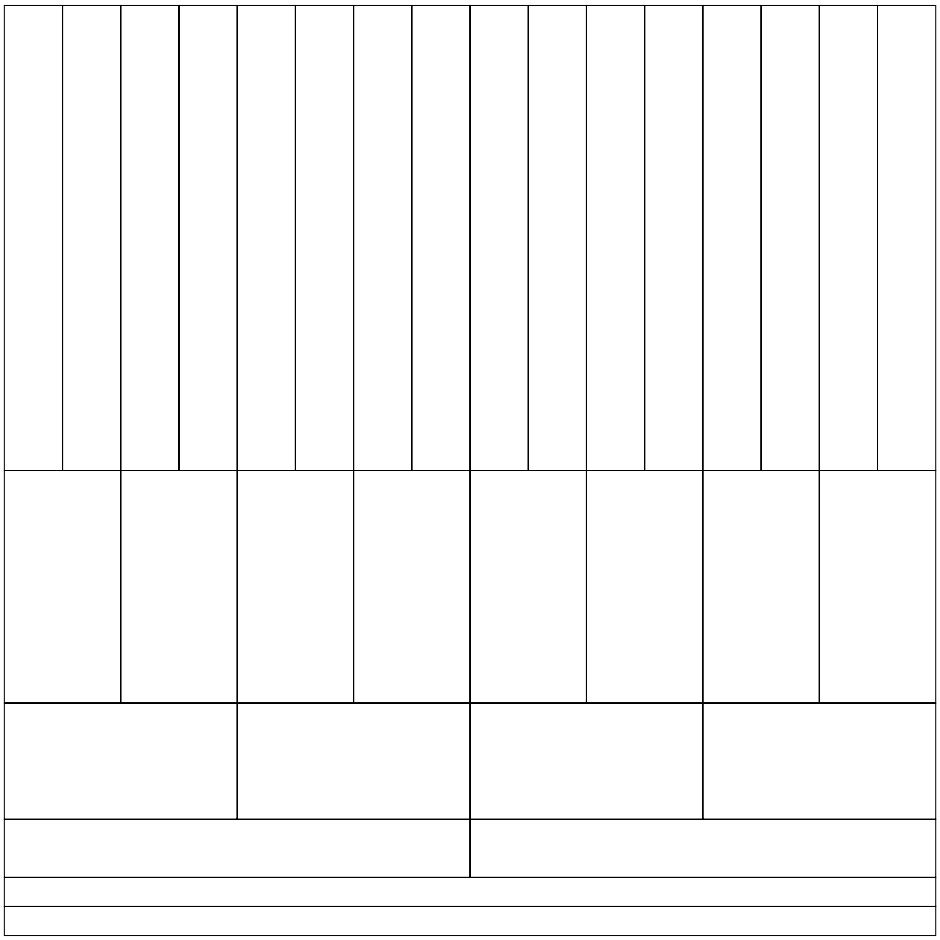

### A.3.2 Examples

Following are certain canonical signals and their automatic analyses by Xwpl.

We first analyze a relatively smooth transient, spread over 9 samples in a 256 sample signal (figure A.8).

Notice that the wavelet analysis at the right correctly localizes the peak in the high-frequency components, but is forced to include poorly localized low-frequency elements as well. The best-basis analysis finds the optimal representation within the library, which in this case is almost a single wavelet packet.

The second signal is taken from a recording (at 8012 samples per second) of a person whistling (figure A.9), using WPLab, the NeXTstep equivalent of Xwpl.

Here the wavelet basis is only able to localize the frequency within an octave, even though the best-basis analysis shows that it falls in a much narrower band. The vertical stripes among the wavelet Heisenberg boxes may be used to further localize the frequencies, but the best-basis decomposition performs this analysis automatically.

Let us now combine the transient and periodic parts in different ways. For example, we may take a critically damped oscillator which receives an impulse, and decompose the resulting solution in the wavelet and best-level bases, as in figures A.10 and A.11. The wavelet decomposition locates the discontinuity at the impulse, while the best-level analysis finds the resonant frequency of the oscillator more precisely.

The exponential decay of the amplitude is visible in both analyses.

A chirp is an oscillatory signal with increasing modulation. Take for example the functions $\sin(.0016t^2)$ and $\sin(10^{-6}t^3)$ on the interval $0 < x < 1024$, sampled 1024 times (figure A.13). The modulation increases linearly and quadratically, respectively. The Heisenberg boxes form a line and a parabolic arc, respectively. In the best-level analyses, all the Heisenberg boxes have the same aspect ratio, which is appropriate for a line. In the best-basis analysis, the Heisenberg boxes near the zero-slope portion have smaller aspect ratio than those near the large-slope portion.

Such a time-frequency analysis can separate superposed chirps. In figure A.14 are pairs of linear chirps, differing either by modulation law or phase. Both are functions on the interval $0 < t < 1024$, sampled 1024 times. On the left is the function $\sin(.0016t^2) + \sin(.0008t^2)$ analyzed in the best wavelet

Figure A.8: Representing a Fast Transient

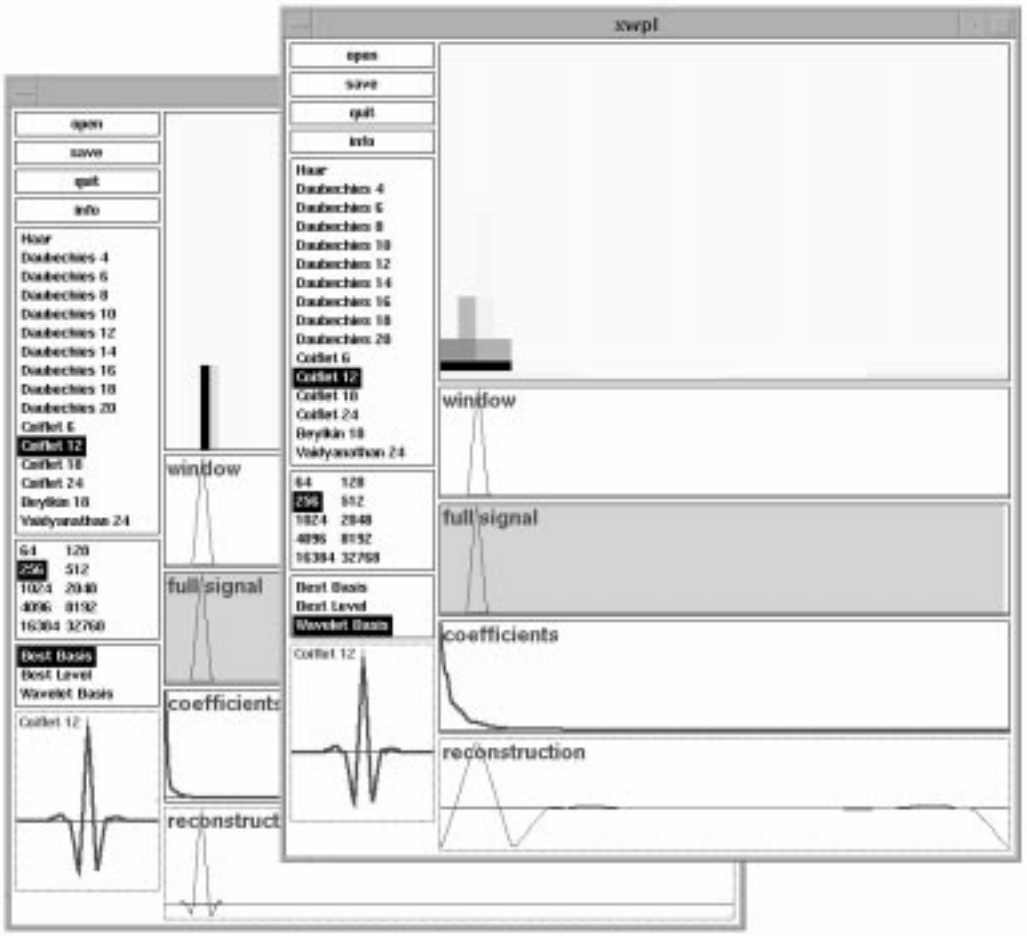

Figure A.9: Representing a Whistle

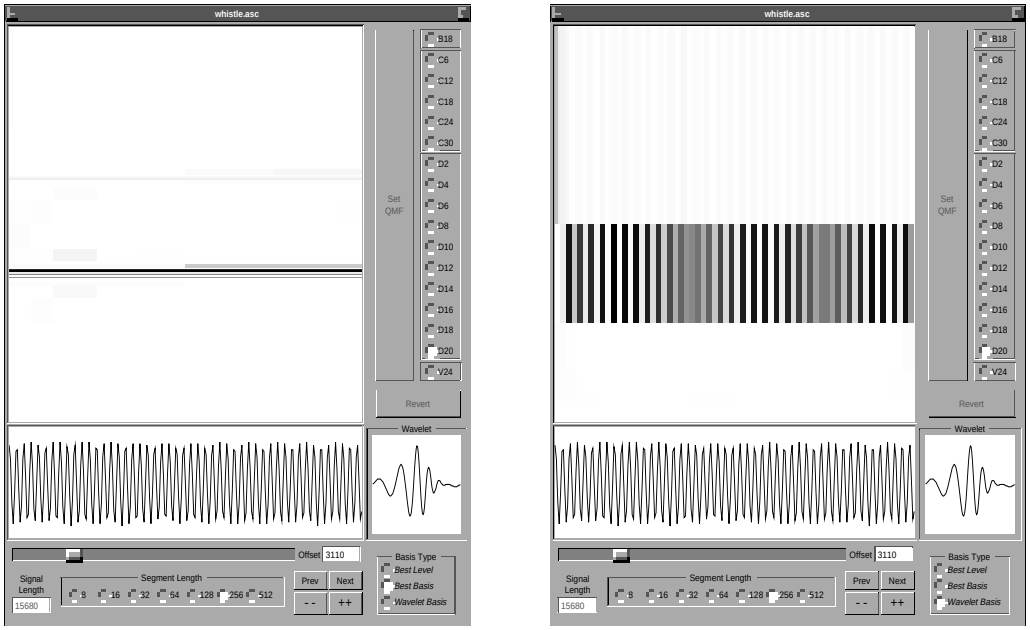


*Best basis*

*Wavelet basis*

Figure A.10: Critically Damped Harmonic Oscillator (Wavelet Basis)

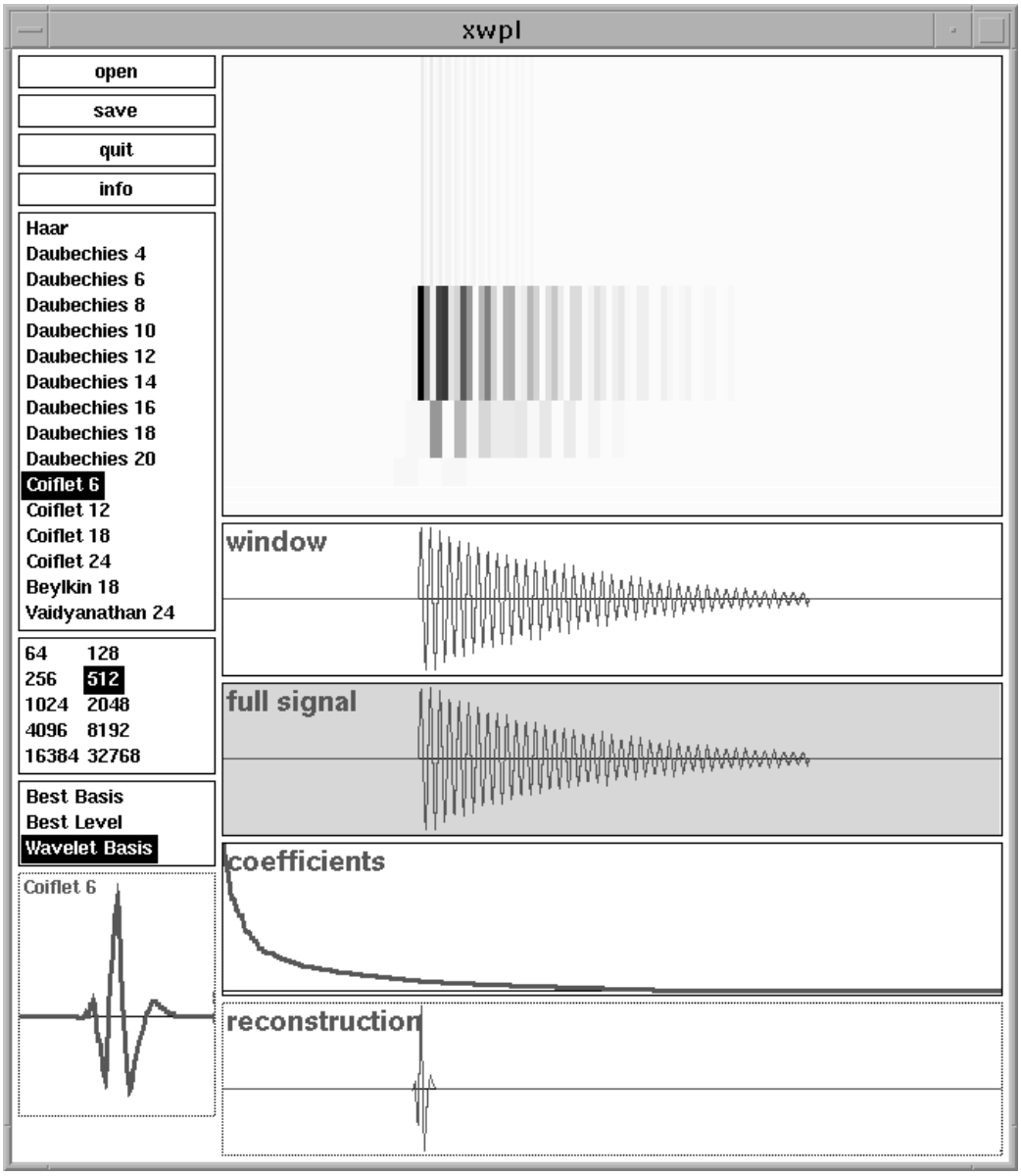

Figure A.11: Critically Damped Harmonic Oscillator (Best Level)

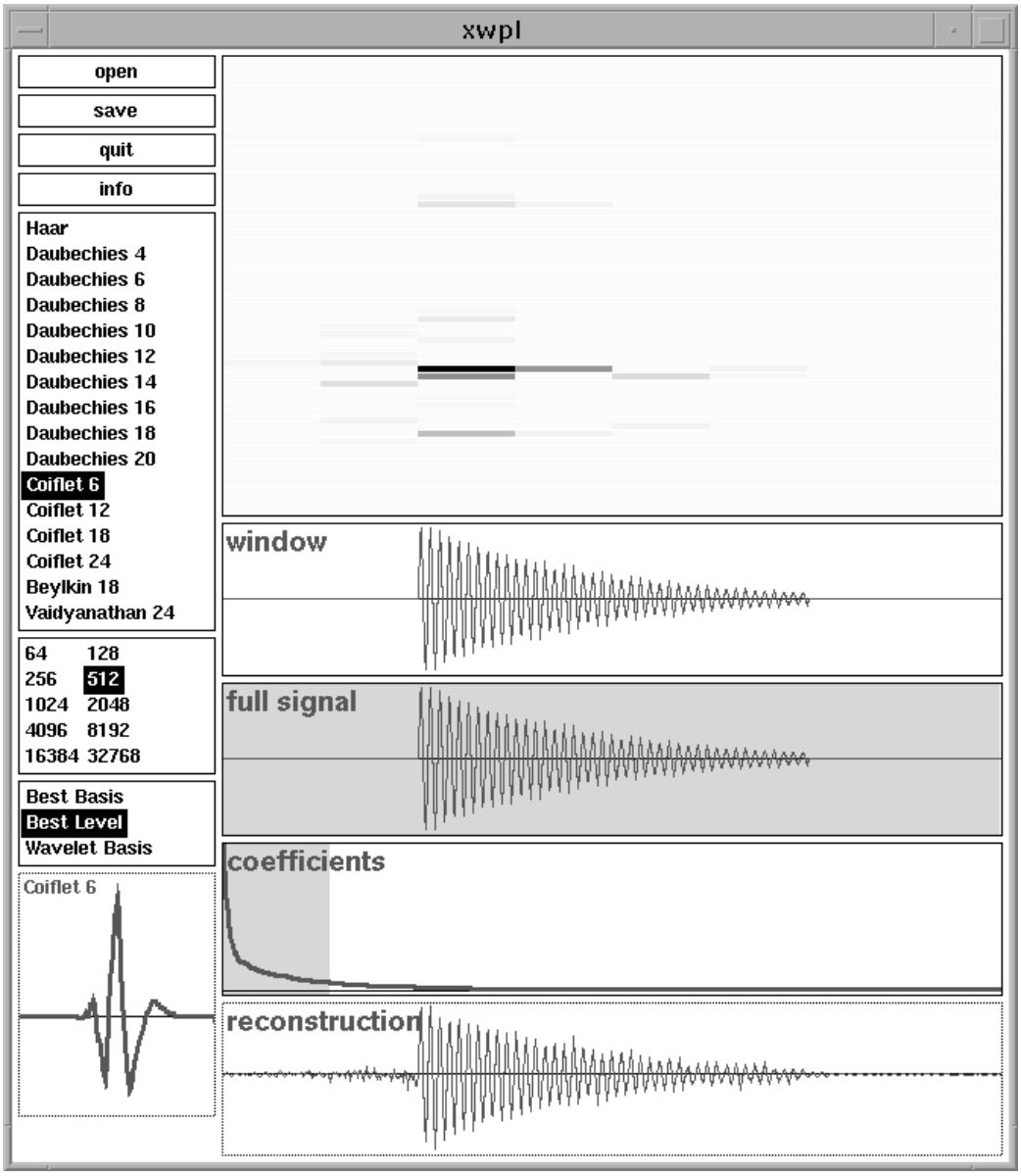

Figure A.12: Critically Damped Harmonic Oscillator (Best Basis)

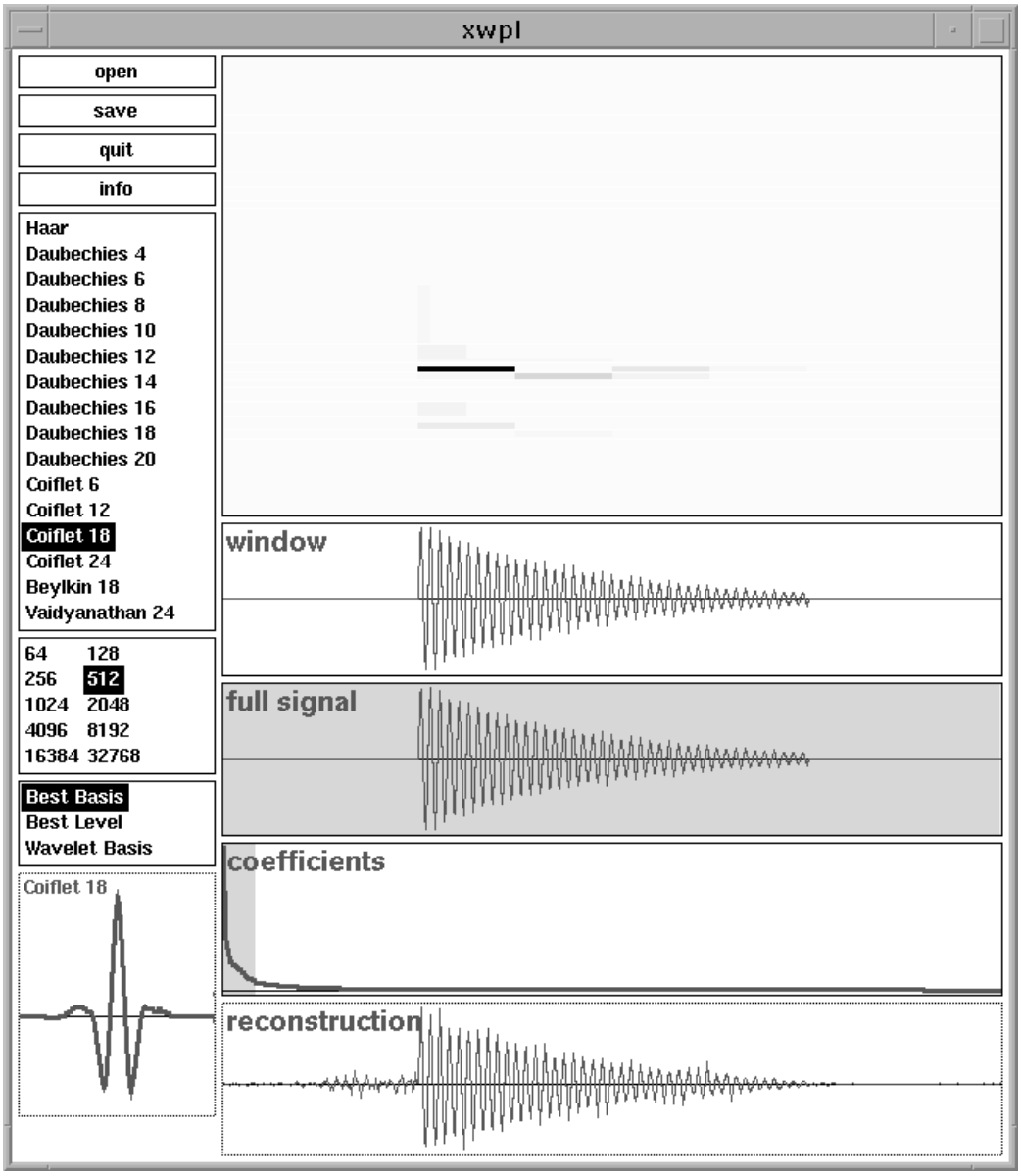

Figure A.13: Linear and Quadratic Chirps

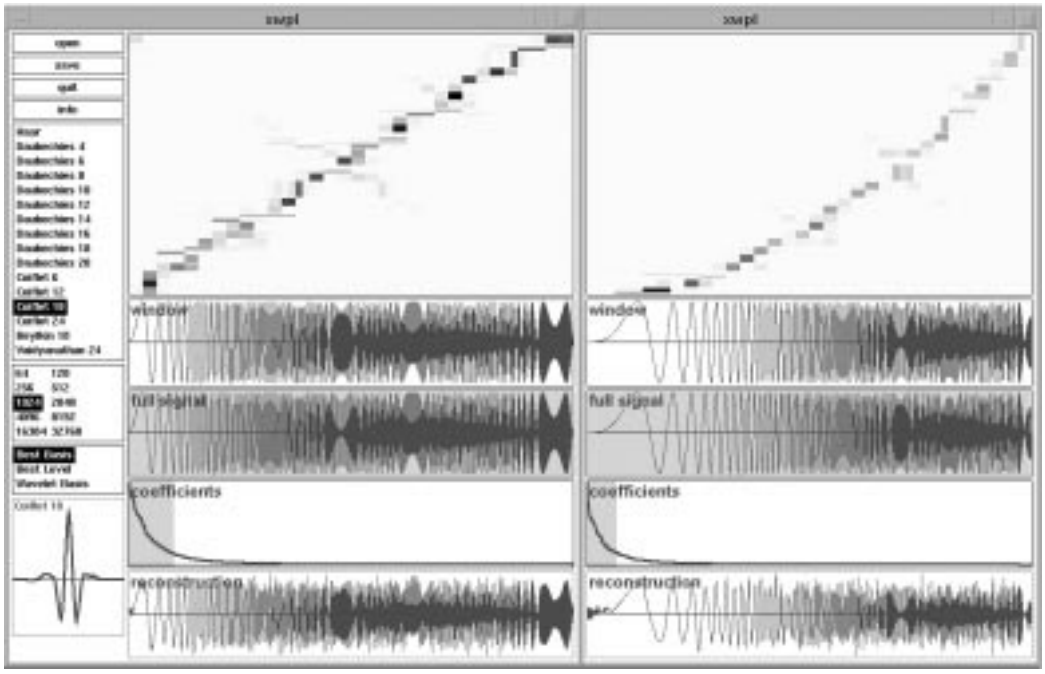

Figure A.14: Superposed Chirps

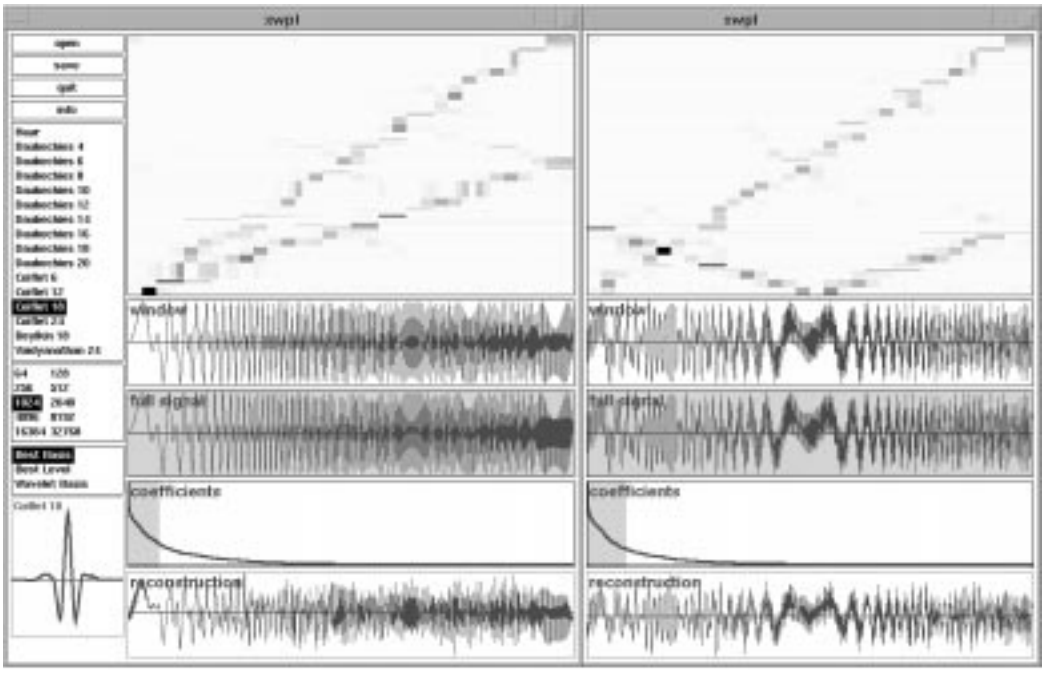


packet basis. Note that the milder slope chirp is represented by Heisenberg boxes of lower aspect ratio. On the right is $\sin(.0016t^2)+\sin(.0016(t-512)^2)$, analyzed by best-level wavelet packets. The downward-sloping line comes from the aliasing of negative frequencies.

## A.4 The Haar System

## A.5 The Haar basis

The Haar wavelet is defined as:

$$h(x) = \begin{cases} 1 & 0 < x \leq \frac{1}{2} \\ -1 & \frac{1}{2} < x \leq 1 \\ 0 & x \leq 0 \text{ or } 1 < x \end{cases}$$

The Haar basis, consisting of the functions

$$h_k^j(x) = 2^{j/2} h(2^j x - k) \qquad \begin{matrix} j=0,\pm1,\pm2\ldots \\ k=0,\pm,\pm2\ldots \end{matrix}$$

that is rescaled versions of $h(x)$ (by $2^j$) shifted by $2^{-j}k$. These functions are orthogonal i.e.

$$\langle h_k^j, h_{k'}^{j'} \rangle \equiv \int h_k^j(x) h_{k'}^{j'}(x) dx = \begin{cases} 1 & \text{if } j = j' \quad k = k' \\ 0 & \text{otherwise} \end{cases}$$

Moreover, they form a basis for all functions $f$ with finite square integral $\int_{-\infty}^{\infty} \|f(x)\|^2 dx < \infty$. This means that we can represent such a function as

$$f(x) = \sum_{j,k} \langle f, h_k^j \rangle h_k^j(x).$$

The coefficients $d_k^j = \langle f, h_k^j \rangle$ are called the Haar Wavelet coefficients.

In order to facilitate the transition between the functions (continuous) point of view and the discrete (sample) numerical approach we choose to discretize a function on a given scale by defining its "sampled" values as being averages on that scale, i.e. for a fixed $j$ we define

$$s_k^j = 2^{j/2} \int_0^{2^{-j}} f(x + 2^{-j}k) dx = \langle f, \chi_k^j \rangle$$

where

$$\chi(x) = \begin{cases} 1 & 0 < x \leq 1 \\ 0 & x \leq 0 \text{ or } 1 \leq x \end{cases}$$

is called a scaling function $\chi_k^j(x) = 2^{j/2}\chi(2x^j - k)$ (the function is normalized so that $\langle \chi_k^j, \chi_k^j \rangle = 1$). The number $2^{j/2} s_k^j$ is the average of $f$ on the interval $[2^{-j}k, 2^{-j}(k+1)]$.

We observe that $d_k^{j-1} = \frac{1}{\sqrt{2}}(s_{2k}^j - s_{2k+1}^j)$, from which we deduce the recursive algorithm for computing the Haar coefficients in figure A.15.

Figure A.15: Recursive algorithm for the Haar coefficients

$$\begin{array}{ccccccccc} s^0 & \longrightarrow & s^1 & \longrightarrow & s^2 & \longrightarrow & s^3 & \cdots \\ & \searrow & & \searrow & & \searrow & & \\ & & d^1 & & d^2 & & d^3 & \cdots \end{array}$$

$$\text{with} \quad s_k^{j-1} = \frac{1}{\sqrt{2}}(s_{2k}^j + s_{2k+1}^j)$$

Interpretation: $s_k^j$ represent the time average of the signal $f$ on $k^{\text{th}}$ time intervals of length $2^{-j}$, $d_k^j$ represent the variation of the average time signal on two consecutive intervals.

### A.5.1 Haar Multiscale Analysis

We observe that for $j$ fixed the function $\chi_k^j$ are mutually orthogonal as $k$ varies and that the map

$$f \to \sum_k \langle f, \chi_{jk} \rangle \chi_{j,k}(x) = P^j(f)$$

is the orthogonal projection on the space of functions which are constant on the intervals

$$(2^{-j}k, 2^{-j}(k+1)) \qquad \text{of length} \quad 2^{-j}$$

(the sampling map). We will call this space $V_j$ and observe that

$$\begin{array}{ll} V_j \supseteq V_{j+1} \supseteq V_{j+2} \cdots & \\ \cup V_j = L^2 & \cap V_j = \{0\} \end{array}$$

if $f \in V_J$. Then $f(2x) \in V_{j+1}$. We also observe that the orthogonal complement of $V_j$ in $V_{j+1}$ is spanned by the Haar wavelets. We will write

$$V_{j+1} = V_j \oplus W_j.$$

### A.5.2 Exercise

Show that $P_{j+1}(f) - P_j(f) = \sum_k \langle f, h_k^j \rangle h_k^j$.

We denote $P_{j+1} - P_j = Q_j$ or $P_{j+1} = P_j + Q_j$. We see that $Q_j$ provides the detail needed to refine the sampling from the averages on scale $j$ $(2^{-j})$ to the scale $j+1$ $(2^{-j-1})$. More generally,

$$P_N = P_0 + Q_0 + Q_1 + Q_2 \cdots Q_{N-1}.$$

- $P_0$ is the average signal on intervals of length 1.
- $Q_0$ addsthe detail to obtain averages on intervals of length $\frac{1}{2}$.
- $Q_1$ adds refinements to intervals of length $\frac{1}{4}$, etc.

### A.5.3 Walsh Functions

We now review the method for computing Haar coefficients: we restrict our attention to a sequence of eight samples $x_1, x_2, \ldots, x_8$ (which can be thought of as averages on intervals of length $\frac{1}{8}$ of a function defined on $[0,1]$). The first computation involved

$$\begin{aligned} s_1 &= \frac{1}{\sqrt{2}}(x_1 + x_2) = \frac{1}{\sqrt{2}}(x_1, x_2, \ldots, x_8) \cdot (1, 1, 0 \ldots 0) \\ d_1 &= \frac{1}{\sqrt{2}}(x_1 - x_2) = \frac{1}{\sqrt{2}}(x_1, x_2, \ldots, x_8) \cdot (1, -1, 0, \ldots 0) \\ s_2 &= \frac{1}{\sqrt{2}}(x_3 + x_4) = \frac{1}{\sqrt{2}}(x_1, x_2, \ldots, x_8) \cdot (0, 0, 1, 1, 0 \ldots 0) \\ d_2 &= \frac{1}{\sqrt{2}}(x_3 - x_4) = \text{etc}\ldots \end{aligned}$$

Observe that the transformation from $x$ to $\{s\}$ and $\{d\}$ consists of a string of rotations by $\frac{\pi}{4}$ of the vectors $(x_1, x_2)(x_3, x_4) \ldots$. Therefore, $x_1^2 + x_2^2 \ldots x_8^2 = s_1^2 + s_2^2 + s_3^2 + s_4^2 + d_1^2 + d_2^2 + d_3^2 + d_4^2$, i.e. the total energy is conserved.

In the second stage we view $s_1 s_2 s_3 s_4$ as new samples (they are "averages" on intervals of length $\frac{1}{4}$) and repeat the procedure, computing sums of sums $ss_1$ $ss_2$ and differences of sums $ds_1$ $ds_2$.

It is natural to also view the differences $d_1 \ldots d_4$ (which measure the variation of the samples) as a new signal and perform the same transformations on them.

$sd_1$ $sd_2$ corresponding to average variation.

$dd_1$ $dd_2$ corresponding to change in variation.

and continuing to fill in the rectangle, row by row, as in figure A.16.

Figure A.16: A rectangle of Haar wavelet packet coefficients

| $x_1$ | $x_2$ | $x_3$ | $x_4$ | $x_5$ | $x_6$ | $x_7$ | $x_8$ |
|---|---|---|---|---|---|---|---|
| $s_1$ | $s_2$ | $s_3$ | $s_4$ | $d_1$ | $d_2$ | $d_3$ | $d_4$ |
| $ss_1$ | $ss_2$ | $ds_1$ | $ds_2$ | $sd_1$ | $sd_2$ | $dd_1$ | $dd_2$ |
| $sss_1$ | $dss_1$ | $sds_1$ | $dds_1$ | $ssd_1$ | $dsd_1$ | $sdd_1$ | $ddd_1$ |

(This procedure will be interpreted later as subband coding).

Figure A.17: Haar wavelet packets on $\mathbb{R}^8$:

Smallest scale = level 1;
Intermediate scale = level 2;
Largest scale = level 3.

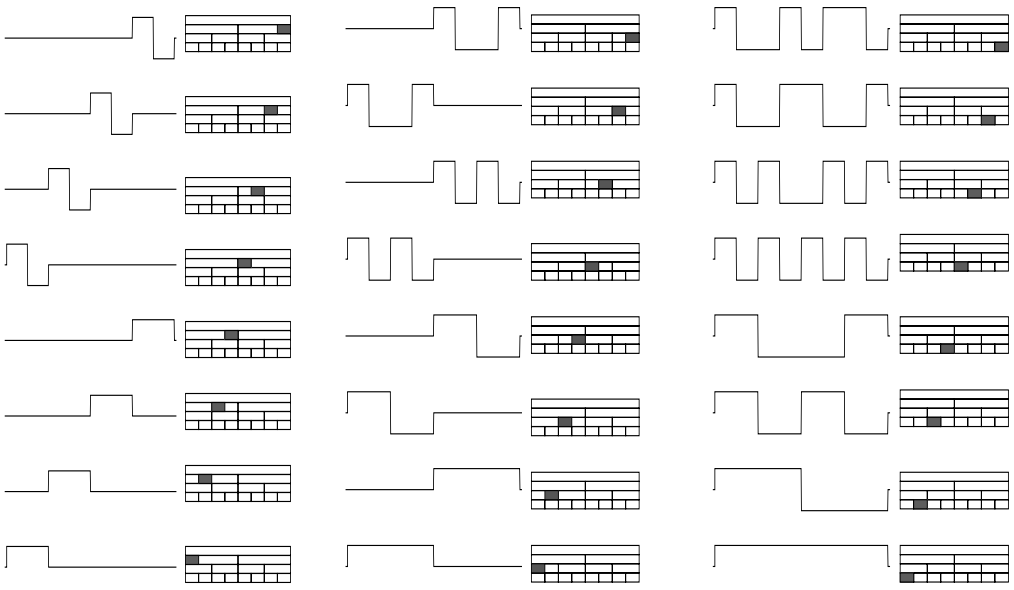

We observe that each entry in this rectangular array of numbers represents an inner product of the original signal $(x_1, \ldots, x_8)$ with a multiple of a vector with entries $\pm 1$ as described in the following diagrams:

For example, the entry $dd_1$ is obtained by taking

$$\begin{aligned}\frac{1}{\sqrt{2}}(d_1 - d_2) \qquad &= \tfrac{1}{2}(x_1, x_2, \ldots, x_8)(1, -1, 0, 0, \ldots 0) \\ &\quad -\tfrac{1}{2}(x_1, x_2, \ldots, x_8)(0, 0, 1, -1, \ldots 0) \\ &= \tfrac{1}{2}(x_1, x_2, \ldots, x_8)(1, -1, -1, 1, 0, 0, 0, 0)\end{aligned}$$

which is the pattern corresponding to the first box in the $4^{\text{th}}$ block on level 2 (the signal is on level 0).

The patterns (or vectors) generated in the preceding pages can be combined in different ways to construct orthogonal basis of eight dimensional space.

The last eight patterns on level 3 represent the well known Walsh pattern functions (providing a square wave Fourier analysis). Clearly the transform mapping the original sequence into the entries of the bottom row is orthogonal (since it was obtained by a succession of orthogonal transformations). Therefore the different patterns which are the columns of this transformation are orthogonal. The basis corresponding to a fixed row provides a windowed Walsh transform.

The discrete Haar wavelet basis is obtained by choosing the second block in each row and the first and second entry on the last row.

It is easy to see that any collection of blocks in the rectangle with the property that their shadow intervals form a disjoint cover of the full range provides a collection of patterns forming a basis. As can be seen on the following example diagram, we use the entries on the bottom level (3) to recover the entries on the "parent" box above these entries. We then use the entries on level 2 to recover all entries on level in the parent box. We now have a full set of entries on level one enabling us to recover the original signal. Since all transformations were orthogonal we must have that the collection of vectors corresponding to this choice of patterns is an orthogonal basis of $\mathbb{R}^8$.

## A.6 General wavelet packets

We'll use the notation and terminology of [2], whose results we shall assume.

We are given an exact quadrature mirror filter $h(n)$ satisfying the conditions of Theorem (3.6) in [2], p. 964, i.e.

$$\sum h(n-2k)h(n-2\ell) = \delta_{k,\ell}\ ,\ \sum h(n) = \sqrt{2}.$$

We let $g_k = h_{k+1}(-1)^k$ and define the operations $F_i$ on $\ell^2(\mathbb{Z})$ into "$\ell^2(2\mathbb{Z})$"

$$\begin{aligned} F_0\{s_k\}(i) &= 2\sum s_k h_{k-2i} \\ F_1\{s_k\}(i) &= 2\sum s_k g_{k-2i}. \end{aligned} \tag{A.1}$$

The map $F(s_k) = F_0(s_k) \oplus F_1(s_k) \in \ell^2(2\mathbb{Z}) \oplus \ell^2(2\mathbb{Z})$ is orthogonal and

1.1 $$F_0^* F_0 + F_1^* F_1 = I$$

We now define the following sequence of functions.

$$\begin{cases} W_{2n}(x) = \sqrt{2}\sum h_k W_n(2x-k) \\ W_{2n+1}(x) = \sqrt{2}\sum g_k W_n(2x-k) \end{cases}$$

Clearly the function $W_0(x)$ can be identified with the function $\varphi$ in [**D**] and $W_1$ with the function $\psi$.

Let us define $m_0(\xi) = \frac{1}{\sqrt{2}}\sum h_k e^{-ik\xi}$ and

$$m_1(\xi) = -e^{i\xi}\bar{m}_0(\xi+\pi) = \frac{1}{\sqrt{2}}\sum g_k e^{ik\xi}$$

All of the functions $W_n$ have a fixed scale, but we observe that mixed-scale decompositions of $L^2$ are also possible. This allows us to refine the decomposition $L^2$ by scales as embodied in the following:

**Theorem 1** *For every partition $P$ of the nonnegative integers into sets of the form $I_{kn} = \{2^k n, \ldots, 2^k(n+1)-1\}$, the collection of functions $\{2^{k/2}W_n(2^k t - j) : I_{kn} \in P, j \in \mathbb{Z}\}$ is an orthonormal basis for $L^2(\mathbb{R})$.*

### A.6.1 Remark

We may also think of $I_{nk}$ as the dyadic subinterval $[2^{-k}n, 2^{-k}(n+1))$ of $[0,1)$. Such an indexing convention gives a faithful correspondence between disjoint dyadic decompositions of the frequency line and orthonormal wavelet packet subsets of $L^2$.

**Definition 1** *A wavelet packet basis of $L^2(\mathbb{R})$ is any orthonormal basis selected from among the functions $2^{k/2}W_n(2^kt - j)$.*

Beside the Walsh-type basis , examples of wavelet packet bases include the *wavelet basis* and the *subband basis*

A useful picture of the tree of wavelet packet coefficients is that of a rectangle of dyadic blocks. The row number within the rectangle indexes the scale of the wavelet packets listed therein. The column number indexes both the frequency and position parameters. We may choose to group the wavelet packets either by position or by frequency. Grouping by position fills each row of the rectangle with adjacent windowed spectral transforms, analogous to windowed FFT, with the window size determined by the row number and the window position corresponding to the location of the group. The frequency parameter increases within the group.

We will group the coefficients by frequency, since that gives a more efficient implementation, and since the transformation to the other form is obvious. The boxes of coefficients in the rectangle correspond to the decomposition of $\delta^L\Omega_0$ into the subspaces $\delta^k\Omega_n$, for $0 \le k \le L$ and $0 \le n < 2^{L-k}$. The top box corresponds to $\delta^L\Omega_0$, the bottom boxes correspond to $\Omega_n$, for $0 \le n < 2^L$, and box $n$ on level $k$ (counting the bottom as level 0) corresponds to subspace $\delta^k\Omega_n$.

For definiteness we recall the Haar example. Consider a function defined at 8 points $\{x_1, \ldots, x_8\}$, i.e., a vector in $\mathbb{R}^8$. Then the (periodized) wavelet packet coefficients of this function look like figure A.18.

Figure A.18: A rectangle of wavelet packet coefficients.

| | | | | | | | |
|---|---|---|---|---|---|---|---|
| $x_1$ | $x_2$ | $x_3$ | $x_4$ | $x_5$ | $x_6$ | $x_7$ | $x_8$ |
| $s_1$ | $s_2$ | $s_3$ | $s_4$ | $d_1$ | $d_2$ | $d_3$ | $d_4$ |
| $ss_1$ | $ss_2$ | $ds_1$ | $ds_2$ | $sd_1$ | $sd_2$ | $dd_1$ | $dd_2$ |
| $sss_1$ | $dss_1$ | $sds_1$ | $dds_1$ | $ssd_1$ | $dsd_1$ | $sdd_1$ | $ddd_1$ |

Each row is computed from the row above it by one application of either $F_0$ or $F_1$, which we think of as "summing" ($s$) or "differencing" ($d$) operations, respectively. Thus, for example, the subblock $\{ss_1, ss_2\}$ comes from the application of $F_0$ to $\{s_1, s_2, s_3, s_4\}$, while $\{ds_1, ds_2\}$ comes similarly from $F_1$. The two descendent $s$ and $d$ subblocks on row $n+1$ are determined by their mutual parent on row $n$, which conversely is determined by them through the adjoint anticonvolutions $F_0^*$ and $F_1^*$.

The algorithm produces Haar wavelet packets in the "Paley" or "natural" order. The algorithm may be easily modified to produce "sequency" ordered wavelet packets: what is needed is to exchange $F_0$ and $F_1$ whenever the parent's sequency is odd.

Sequency has a strict definition only for Walsh functions, where it is the number of zero-crossing of a function which takes only the values 1 and $-1$. The $n$th Shannon wavelet packet, in sequency order, is band-limited to the intervals $\pm[n, n+1)$. If we define the appropriate notion of "main frequency" in the intermediate case of smooth, compactly supported wavelet packets, we see that main frequency increases monotonically with sequency order.

Paley order can also be obtained from sequency order by the Gray code permutation.

## A.7 Denoising

We now present an algorithm for denoising signals adaptively using libraries of orthonormal waveforms (such as wavelet packets and local trigonometric libraries). The method extracts from a signal a coherent part which is well represented by the given waveforms and a noisy or incoherent part which cannot be "well compressed" by the waveforms.

### A.7.1 Starting on the right basis

The first stage of the algorithms consists in selecting for analysis a segment of a signal of length $N$. A group of libraries and bases, say for example the sampling basis, the Fourier basis, the Haar-Walsh wavelet-packets, various QMF Daubechies filters defining smoother wavelet packets, local trigonometric adapted windows in both frequency and time, etc.

A basis in which the signal $f(x)$ has a minimum entropy is selected i.e.

$$f = \sum_{1}^{N} \alpha_i \omega_i(x) \qquad \Sigma \|\alpha_i\|^2 = \|f\|^2 = 1$$

where $\omega_i$ are the orthogonal waveforms in the selected "best basis" for which

$$\varepsilon(f) = \sum_{1}^{N} \|\alpha_i\|^2 \log_2 \frac{1}{\|\alpha_i\|^2}$$

is minimal.

We recall that $\varepsilon(f)$ is a measure of concentration of the expansion while $d(f) = 2^{\varepsilon(f)}$, called the theoretical dimension represents the "number" of "free" parameters present in the signal

$$c(f) = \frac{d(f)}{N}$$

is the theoretical rate of "compression" achieved by the expansion in $\omega_i(x)$, $0 < c(f) \leq 1$.

### A.7.2 Asymptotics

We observe that if $\alpha_i$ are samples of a random variable with mean 0, variance $\sigma$ with distribution $p(t)$, then

$$\begin{aligned} \varepsilon(f) = \sum_{1}^{N} \frac{\alpha_i^2}{\|f\|^2} \log_2 \left( \frac{\|f\|^2}{\alpha_i^2} \right) &= \frac{1}{N} \sum_{1}^{1} \frac{\alpha_i^2}{(\|f\|^2/N)} \log_2 \frac{2}{\alpha_i^2} \\ &+ \log_2 \left( \frac{\|f\|^2}{N} \right) + \log_2(N) \end{aligned}$$

and since asymptotically,

$$\sum_{1}^{N} \frac{\alpha_i^2}{N} \to \sigma^2 = \int t^2 p(t) dt$$

we obtain

$$\varepsilon(f) = \log_2 N \int \left( \frac{t}{\sigma} \right)^2 \ell g_2 \left( \frac{t}{c} \right)^2 p(t) dt + \varepsilon_N$$

where $\varepsilon_N \to 0$ as $N \to \infty$. Therefore

$$c(f) \sim 2^{-\delta} \qquad \delta = \int \left(\frac{t}{\sigma}\right)^2 \log_2 \left(\frac{t}{\sigma}\right)^2 p(t)dt$$

**Example** (Gaussian distribution):

$$\int_{-\infty}^{\infty} \log_2(t^2) t^2 \frac{e^{-t^2/2}}{\sqrt{2\pi}} dt \simeq 1.052 \Rightarrow c(f) \simeq 0.4823$$

### A.7.3 The selection algorithm

We chose to view a signal $f$ as being noisy or incoherent relative to the basis $\omega_i$ if its entropy is of the same order of magnitude as $\log_2 N - \delta$ giving a poor compression rate $2^{-\delta}$, leading us to the following method.

Start with a signal $f$ of length $N$, find the best basis in each library and select among them the basis minimizing $\varepsilon(f)$. Reorder the coefficients $\alpha_i$ in decreasing order $\alpha_1 \geq \alpha_2 \geq \cdots \alpha_{N_0} > 0$ where $\alpha_i$ for $i \geq N_0$ are all below a precision threshold (say 0.1% of energy). Then decompose

$$f = c_M + r_M \quad \text{where} \quad c_M = \sum_1^M \alpha_i \omega_i, \quad r_M = \sum_{M+1}^{N_0} \alpha_i \omega_i$$

We will say that $c_M$ is coherent and $r_M$ is incoherent if $c(r_M) \geq \tau_0$

The threshold $\tau_0$ is chosen to determine if the compression of $r_M$ using $\omega_i$ is unacceptably bad. We proceed by testing $r_1 r_2 \ldots$ until we reach $M$ for which

$$c_M \geq \tau_0 > 0, \qquad 0 < \tau_0 < 1$$

or

$$\sum_{i=M_0+1}^{N_0} \frac{\alpha_i^2}{\|r_M\|^2} \log_2 \left(\frac{\|r_M\|^2}{\alpha_i^2}\right) \geq \log_2(N_0 - M_0 + 1) - \log_2 \tau_0.$$

We can now consider $r_M$ as a new signal for which we repeat the decomposition, i.e. pick a best basis and decompose

$$r_M = c'_{M_1} + r'_{M_1}$$

iterating a fixed number of times or stopping whenever no new coherent part is obtained.

The Xwpl program automatically determines the threshold using heuristics on the coefficient curve.

# Bibliography


[1] **R. R. Coifman, F. Majid**
Adapted Waveform Analysis and Denoising, Proceedings, International Conference "Wavelets and Applications", Toulouse, France (1992)

[2] **I. Daubechies**
Orthonormal bases of compactly supported wavelets, Communications on Pure and Applied Mathematics, vol XLI, 1988, pages 909–996

[3] **S. Mallat**
Review of Multifrequency Channel Decomposition of Images and Wavelet Models, Technical Report 412, Robotics Report 178, NYU (1988).

[4] **Y. Meyer**
Wavelets and Operators, Analysis at Urbana vol.1 edited by E. Berkson, N.T. Peck and J. Uhl, London Math. Society, Lecture Notes Series 137, 1989

[5] **R. Coifman,Y. Meyer, Steven Quake, M.Victor Wickerhauser**
Signal Processing and Compression With Wavelet Packets, Proceedings Toulouse 1992

[6] **R. Coifman, Y. Meyer, and V. Wickerhauser**
Wavelet Analysis and Signal Processing, Proceedings, conference on Wavelets, Lowell Mass 1991

[7] **R. Coifman and Y. Meyer**
Remarques sur l'analyse de Fourier à fenêtre, C. R. Acad. Sci. Paris, vol 312, série I, 1991, pages 259–261